Hindawi
Advances in Materials Science and Engineering
Volume 2019, Article ID 8758203, 11 pages
https://doi.org/10.1155/2019/8758203

Research Article

Analysis of Changes in the Micromorphology of Sandstone Joint Surface under Dry-Wet Cycling

Jingcheng Fang, Huafeng Deng, Yu Qi, Yao Xiao, Hengbin Zhang, and Jianlin Li

Key Laboratory of Geological Hazards on Three Gorges Reservoir Area (China Three Gorges University), Ministry of Education, Yichang, Hubei 443002, China

Correspondence should be addressed to Huafeng Deng; dhf8010@ctgu.edu.cn

Received 17 October 2018; Accepted 12 December 2018; Published 21 January 2019

Academic Editor: Pietro Russo

Changes in the micromorphology of joint surface under dry-wet cycling have a direct effect on the mechanical properties of the jointed rock masses, which in turn affects the deformation stability of the bank slope of a reservoir. In this study, we design and carry out a test that aims to quantity the effects of repeated rise and fall of a reservoir on the properties of a jointed rock masses. The results are as follows: first, the roughness, local gradient, and undulation of the joint surface gradually decreased under repeated dry-wet cycling. In addition, the height parameters and texture parameters showed a steep decrease followed by a slow decline. The deterioration was particularly obvious over the first 5 dry-wet cycles. Second, the roughness coefficient of the joint surface, the compressive strength of the face wall, and the basic friction angle were gradually reduced under dry-wet cycling. The shear strength of the jointed rock masses (obtained both quantitatively and experimentally) showed a deteriorating trend controlled by the deterioration of the micromorphology, the strength of the face wall, and the frictional properties of the joint surface. Finally, the dry-wet cycling process determined trends of changes in the microstructure parameters and mechanical properties of the joint surface. Our research results provide a good basis for the analysis of the deterioration and failure of rock masses within the hydrofluctuation belt of a bank slope.

1. Introduction

Natural rock masses often have large numbers of microscopic or macroscopic defects such as joint fractures. Under the action of ground stress, these joint fractures are subjected to loads such as extrusion and shear, and the joint surface becomes a key region of stress release or concentration. Joint surface properties often control the stability of the entire rock mass structure. Compared with intact rock itself, the joint fracture network is quite permeable, allowing it to control the direction of groundwater migration [1]. The infiltration and outflow of water molecules lead to undesirable changes in rock mechanical parameters. In addition, they also gradually change the rock microstructure and promote the development of joint fractures and the generation of new joints and cracks. Studies have shown that many rock mass engineering project defects, such as slope and dam foundation instability, are caused by the destruction of structural planes [2] and that more than 90% of slope failures are related to water [3].

As shown in Figure 1, after the completion of the Three Gorges project, reservoir water levels fluctuate within a belt up to 30 m wide, which represents the range between the flood control level (145 m) and the power plant level (175 m). Under conditions of frequent water level fluctuation, the rock masses in the fluctuating belt periodically undergo dewatering and saturation, resulting in a "fatigue effect." The effect of a single cycle may not necessarily be significant, but after repeated cycles, progressive damage can occur [4, 5]. As can be seen from Figure 1, in the area of water fluctuation (145 m to 175 m), there is almost no vegetation. Instead, we clearly see well-developed rock joints and fissures. At the same time, previous studies [5] have shown that under large fluctuations in the reservoir water level, the damaging effect

Figure 1: Diagram of the destruction of rock masses in a typical slope bank.

of dry-wet cycling exists not only on the surface of the slope but also within the internal rock masses, which are affected by groundwater fluctuation. Over time, the changes in the physical and mechanical properties of the jointed rock masses will directly affect the deformation and stability of the reservoir bank slope, and it is likely that the slope will become increasingly unstable over time.

In recent years, more scholars have begun to pay attention to dry-wet cycling along the wading slope in hydropower projects. For example, Wang et al. [4] comprehensively analyzed the types and characteristics of dry-wet cycling in the reservoir area; Liu et al. [5] experimentally simulated the process of dry-wet cycling under fluctuations in reservoir water levels and concluded that the shear strength of sandstone decreases with increases in the number of "saturated-air-dried" water-rock cycles; and Xu [6] found that the water-rock chemical action in the slope area of silicate rocks mainly occurred in the unsaturated zone and the fluctuation zone of the water level. In addition, a series of water-rock tests on sandstone, shale, and mudstone were carried out by many scholars, including Zhou et al. [7], Hale and Shakoor [8], Fu et al. [9, 10], Yao et al. [11], Jiang et al. [12], Guo [13], Apollaro et al. [14], Tallini et al. [15], Alt-Epping et al. [16], Huang [17], Hurowitz and Fischer [18], Cui et al. [19], Zhou [20], Wang [21], Zhang et al. [22], Deng et al. [23, 24], and others. The results of these studies show that dry-wet cycling can cause irreversible progressive damage to the rock masses. Jeng et al. [25] and Lin et al. [26] studied the microscopic mechanism of sandstone degradation under the effect of dry-wet cycling.

Based on the present research results, it is clear that the deterioration of mechanical properties of rock under dry-wet cycling is an important and common process. However, the influence of dry-wet cycling on joints and cracks specifically has rarely been considered. The microscopic topography of joints is the fundamental attribute that affects the mechanical behavior and hydraulic behavior of jointed rock masses. For example, the shear strength and permeability of a joint are determined by the microscopic attributes of those joints. Moreover, dry-wet cycling leads to deterioration of the physical and mechanical properties of the rock masses, a microscopic process with an important macroscopic effect. Therefore, quantitative analysis of the micromorphology of the joint surface under dry-wet cycling provides an accurate basis for understanding dry-wet cycling in rock masses making up the bank slope.

2. Test Scheme

2.1. Preparation of Single Joint Samples. It is very difficult to collect natural jointed rock samples on the site, and the experimental results are difficult to control. Therefore, in this paper, a single sandstone joint sample was prepared artificially. Sandstone is a very typical type of stratified rock. As shown in Figure 1, fractures along the bedding and weak planes of the hydrofluctuation belt are well developed. For this reason, we focus on sandstones with distinctive stratification. The rock blocks retrieved at the site were cut and polished into standard cubes with a side length of 100 mm. Then, each rock sample was split along the weak plane. We selected the resulting specimens with smooth joint surfaces and no local lumps as our single joint rock samples. Typical rock samples are shown in Figure 2. Typical physical and mechanical parameters of sandstone are shown in Table 1.

2.2. Dry-Wet Cycling Test Scheme. As can be seen in Figure 1, the rock body collapse phenomenon in the fluctuating zone of the bank slope is obvious. Therefore, in the experiment, the dry-wet cycling process of the hydrofluctuation belt is simulated. A dry-wet cycle test program was designed. First, the joint rock samples were dried at 105°C for 24 hours, then cooled to room temperature, force-saturated for 4 hours under a vacuum, and finally soaked in water for 24 hours [5]. The process is designed to undergo 20 dry-wet cycles. The block diagram of the dry-wet cycling test scheme is shown in Figure 3.

2.3. Joint Microscopic Scanning Analysis. To facilitate analysis of the influence of dry-wet cycling on the topological characteristics of the joint surface, an ST500 three-dimensional noncontact surface profiler was used to scan the joint surface at the start and end of the dry-wet cycles 1, 3, 5, 8, 12, 16, and 20. As shown in Figure 4, the device uses a front-end laser scanning confocal microscope to test and analyze the sample surface. Three-dimensional image analysis software can then be used to obtain the microtopographic parameters of the sample surface.

3. Analysis of the Variation of Microscopic Topography Characteristics of Joints under Dry-Wet Cycling

The microscopic topography scanning images of the periodic joint surfaces of different dry-wet cycles are shown in Figure 5.

In the microscopic topography analysis of the joint surface, the least squares surface was used as the datum of the topography, and ST500 software was then used to extract the microscopic topographical parameters.

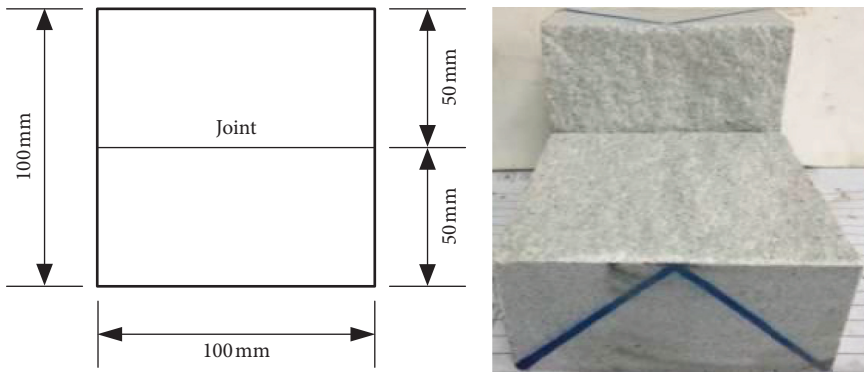

Figure 2: Single joint specimen. (a) Schematic diagram. (b) Well-prepared jointed rock sample.

Table 1: Typical physical and mechanical parameters of sandstone.

Project		Value
Density (g·cm^{-3})	Natural	2.55
	Saturated	2.60
Young's modulus (GPa)		25.6
Poisson's ratio		0.28
Uniaxial compressive strength (MPa)		90
Tensile strength (MPa)		4
Cohesion (kPa)	Natural	390
	Saturated	300
Internal friction angle (°)	Natural	42
	Saturated	34

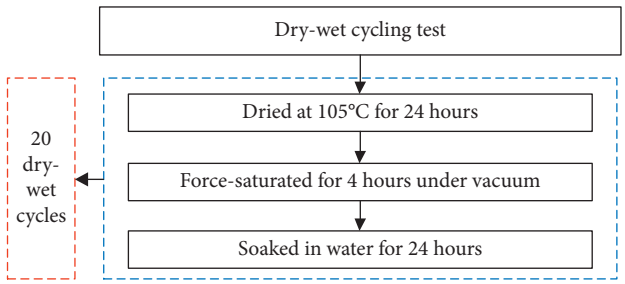

Figure 3: The block diagram of the dry-wet cycling test scheme.

The microstructure parameters of joints usually include height parameters and texture parameters. The height parameter mainly represents the characteristics of the fluctuation of the joint surface, whereas the texture parameter mainly represents the distribution position and correlation of joint points and points.

To make our results comparable with those obtained in previous similar studies [27], we selected 5 height parameters and two texture parameters to be used as the basis of our quantitative statistical analysis of the microscopic features of the joint surface.

The microscopic topography parameters of the periodic joint surface after different numbers of dry-wet cycles are shown in Table 2; the change trends of the microscopic parameters are shown in Figure 6.

To facilitate the comparative analysis of test results, we defined the degree of change in the microscopic topography

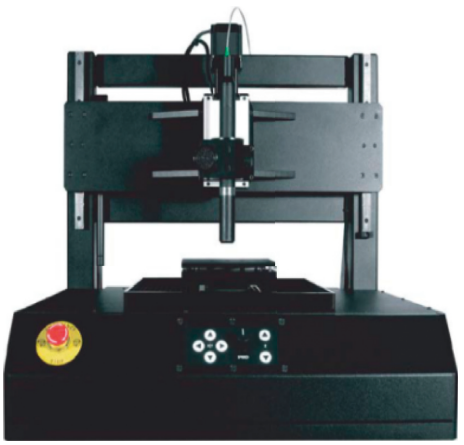

Figure 4: ST500 three-dimensional noncontact surface profiler.

parameters under dry-wet cycling as the degree of deterioration. D_i is the total deterioration degree, and ΔD_i is the deterioration degree of a single dry-wet cycle effect. We calculate D_i and ΔD_i as follows:

$$D_i = \frac{(T_0 - T_i)}{T_0} \times 100\%,$$
$$\Delta D_i = \frac{(D_i - D_{i-1})}{(n_i - n_{i-1})}, \quad (1)$$

where T_0 is the microtopography parameter of the joint surface in the initial state and T_i is the micromorphology parameter of the joint surface after n_i dry-wet cycles. The stage deterioration degree curves of the height parameters and texture parameters are listed in Figure 7.

Table 2 and Figures 6 and 7 allow us to draw the following conclusions:

As the number of dry-wet cycles increases, the height parameters and texture parameters of the joint surface gradually decrease. The trend is steep at first but becomes more gradual as the number of cycles increases. The deterioration degree of joint microscopic topography parameters caused by the first 5 dry-wet cycles is obvious, accounting for 70%–80% of the final deterioration degree.

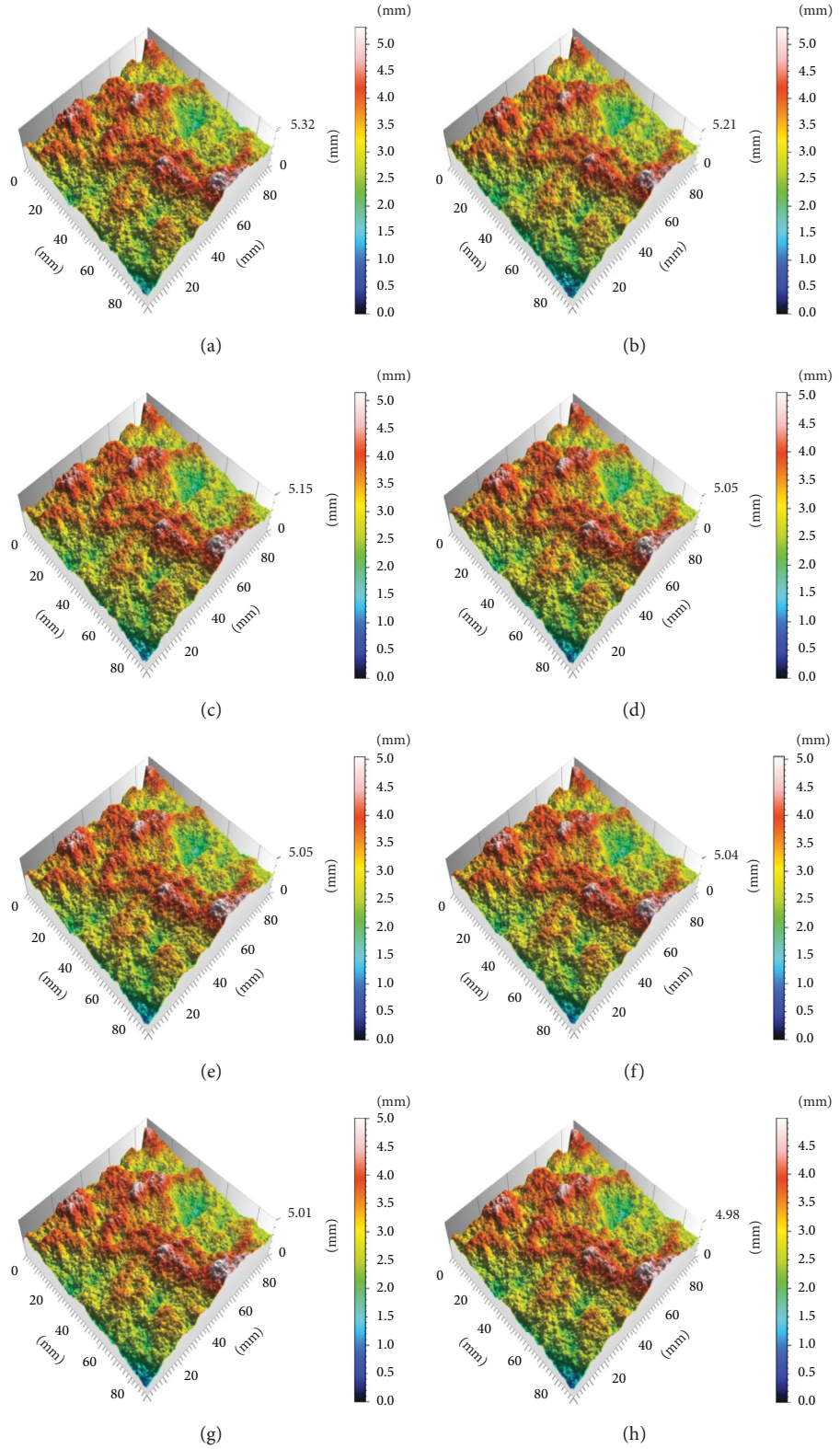

Figure 5: Microscopic topography of joint surfaces under dry-wet cycling. (a) Initial state. (b) 1 dry-wet cycle. (c) 3 dry-wet cycles. (d) 5 dry-wet cycles. (e) 8 dry-wet cycles. (f) 12 dry-wet cycles. (g) 16 dry-wet cycles. (h) 20 dry-wet cycles.

After the first dry-wet cycle, S_p, S_v, S_z, S_a, and S_q decreased by 1.83%, 2.58%, 2.31%, 0.72%, and 0.92%, respectively. After 5 dry-wet cycles, S_p, S_v, S_z, S_a, and S_q decreased by 6.15%, 7.00%, 6.69%, 1.84%, and 2.26%, respectively. After 20 dry-wet cycles, S_p, S_v, S_z, S_a, and S_q decreased by 8.98%, 8.62%, 8.75%, 2.48%, and 2.86%, respectively. The surface maximum peak height S_p represents the distance from the highest point of the surface contour to

Table 2: Microstructure parameters of joint surface under dry-wet cycling.

Number of dry-wet cycles (n)	Maximum surface peak height, S_p (mm)	Maximum surface valley depth, S_v (mm)	Maximum height of contour, S_z (mm)	Arithmetic mean deviation, S_a (mm)	Height mean square root, S_q (mm)	Slope mean square root, S_{dq}	Expand interface area ratio, S_{dr} (%)
0	2.0045	3.4423	5.4468	0.5170	0.6651	0.2612	5.2461
1	1.9678	3.3534	5.3212	0.5133	0.6590	0.2557	5.1803
3	1.9123	3.2345	5.1468	0.5092	0.6523	0.2525	5.0877
5	1.8812	3.2012	5.0824	0.5075	0.6501	0.251	5.0534
8	1.8623	3.1821	5.0444	0.5062	0.6492	0.2495	5.0244
12	1.8434	3.1667	5.0101	0.5050	0.6478	0.2481	4.9878
16	1.8290	3.1523	4.9813	0.5046	0.6466	0.2464	4.9745
20	1.8245	3.1456	4.9701	0.5042	0.6461	0.2458	4.9578

Note. 0 in the table represents the initial state, as explained below.

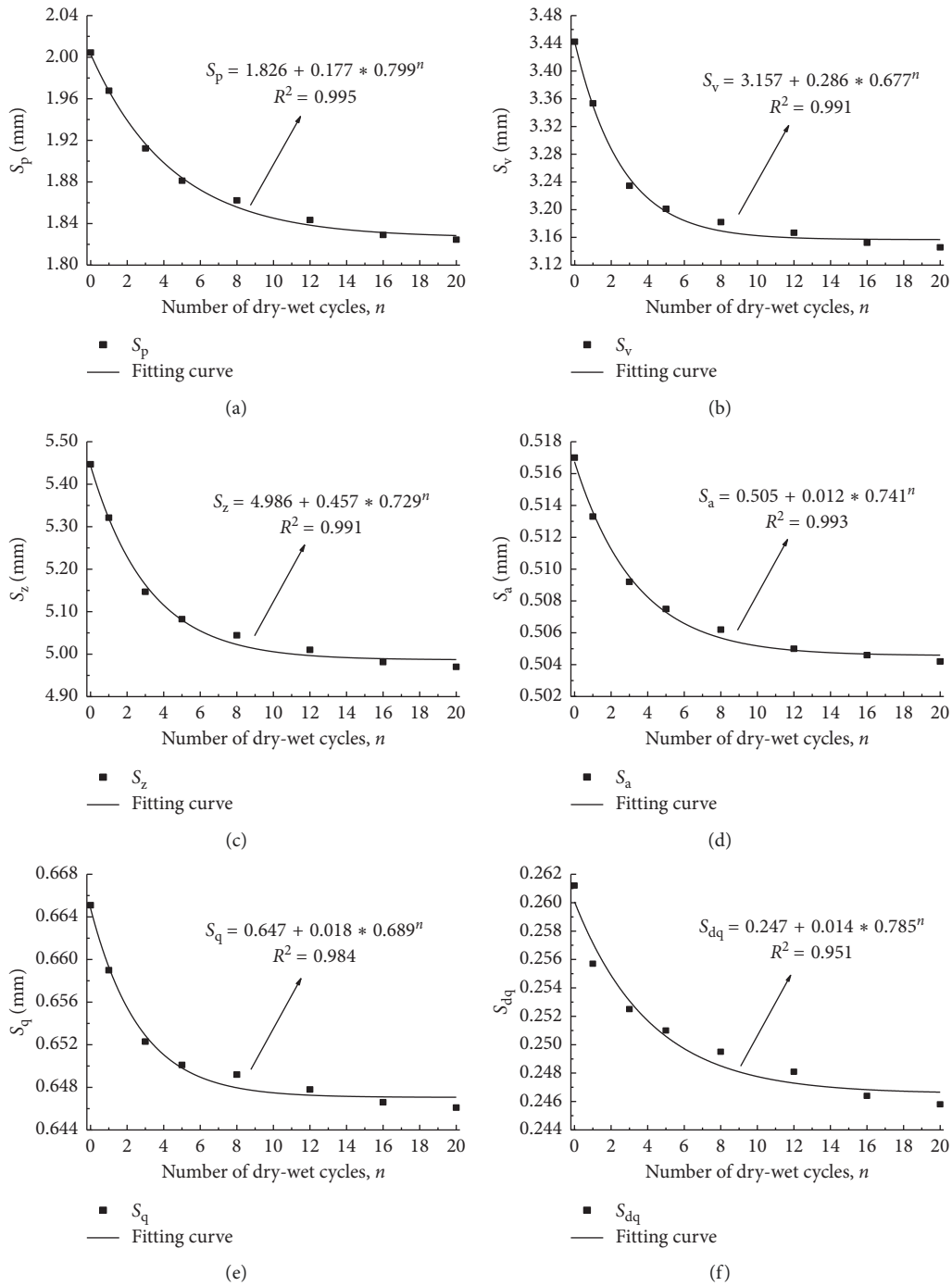

Figure 6: Continued.

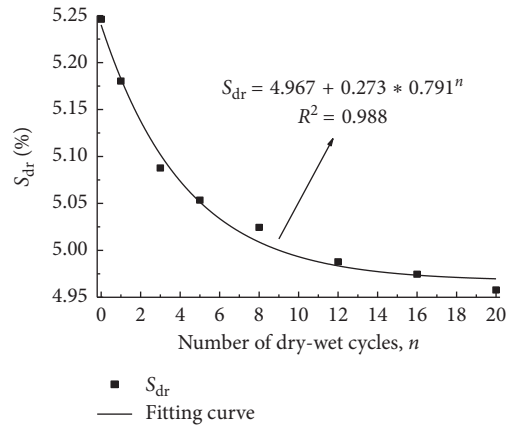

Figure 6: Variations in microstructure parameters of joint surfaces under dry-wet cycling.

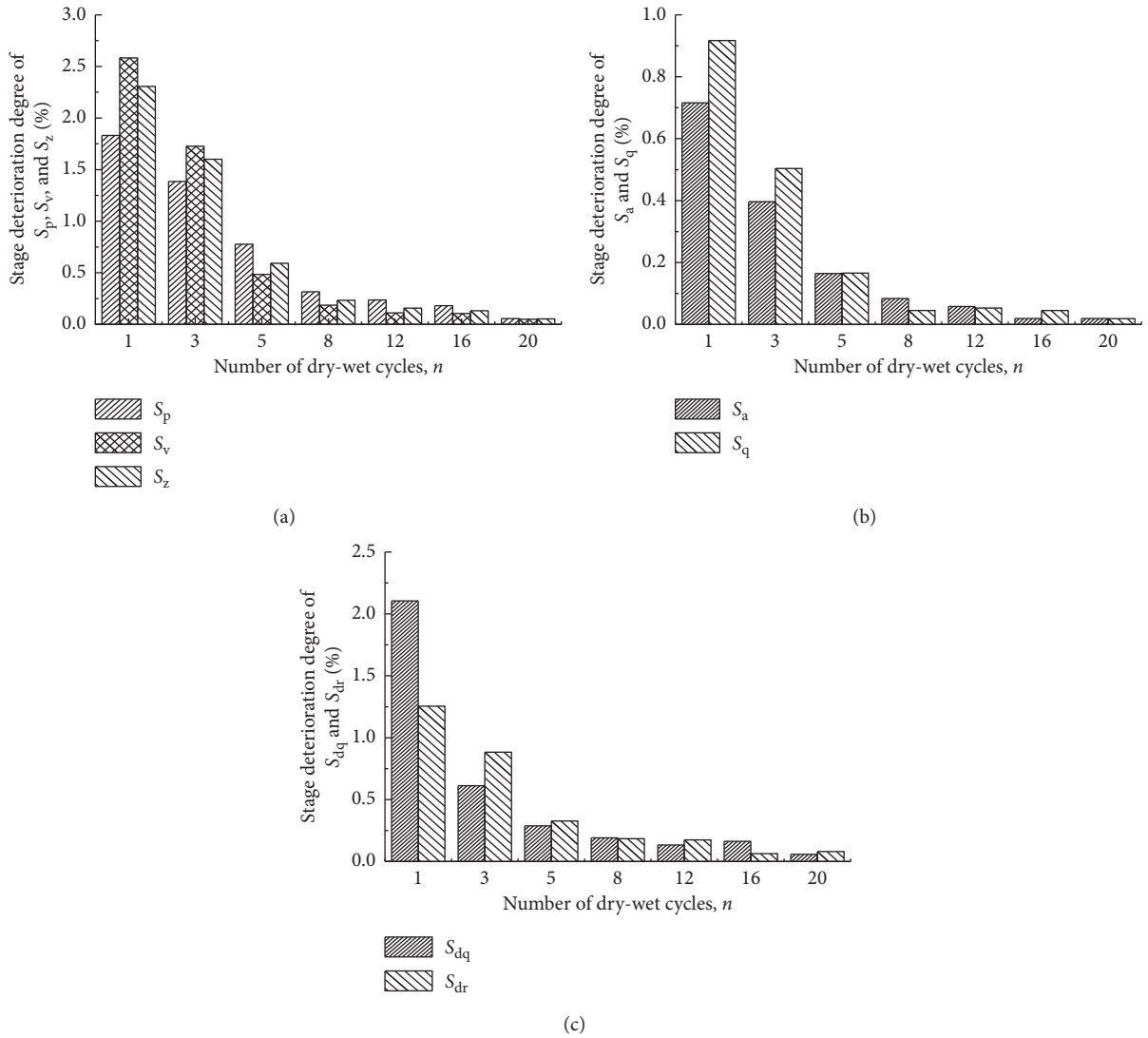

Figure 7: Histogram of the stage deterioration degrees of the microstructure parameters of the joint surface under dry-wet cycling.

the reference plane. The maximum valley depth S_v represents the distance from the lowest point of the surface contour to the reference plane. The maximum height of the contour S_z is the sum of S_p and S_v. Together, these three parameters reflect the maximum peak-to-valley height of the scanned surface. The change rules of S_p, S_v, and S_z indicate that the dry-wet cycle leads to the maximum peak and the maximum valley depth of the joint surface, the joint profile gradually decreases in height, and the overall trend tends to be flat and smooth. The arithmetic mean deviation S_a represents a high degree of deviation between the microscopic topography of the scanning surface and the median plane; it reflects the degree of roughness of the joint surface. The height root mean square root S_q is the square root of the average of the square sum of the distances from the scanning surface point to the reference surface. This value best reflects the discreteness and variability of the microscopic topography of the joint surface. The changing law of S_a and S_q shows that the dry-wet cycling causes the roughness and the fluctuation of the joint surface to gradually decrease. S_{dq} and S_{dr} decreased by 2.11% and 1.25%, respectively, after the first dry-wet cycle. After 5 dry-wet cycles, S_{dq} and S_{dr} decreased by 3.91% and 3.67%, respectively. After 20 dry-wet cycles, S_{dq} and S_{dr} decreased by 5.90% and 5.50%, respectively. The slope root mean square S_{dq} is the root mean square of the first-order reciprocal of the inner contour surface of the scanning surface, which can best reflect the shape and inclination of the joint surface. S_{dr} reflects the complex condition of the scanning surface. In theory, a completely flat surface has a S_{dr} of 0. The larger the S_{dr}, the more complicated the surface conditions. These changes in S_{dq} and S_{dr} show that dry-wet cycling causes the local slope and undulation of the joint surface to gradually decrease.

If changes in the microtopography parameters of the joint surface under dry-wet cycling occur in a continuous manner, we can establish a damage evolution equation describing changes in the microtopography parameters of the joint surface in the presence of dry-wet cycling. We found that the deterioration trend of the microtopography parameters of the joint surface under dry-wet cycling conditions can be described accurately by an exponential function. The fitting curve is shown in Figure 6.

4. Analysis of the Correlation between the Micromorphology and Shear Strength of the Joint Surface

The characteristics of the shear mechanics of jointed rock masses are directly influenced by the micromorphological characteristics of the joint surface. In the past, scholars have analyzed this relationship in terms of the shear strength of a jointed rock masses. Barton proposed an empirical equation for the shear strength of a structural surface [28], which is currently a widely used formula:

$$\tau = \sigma_n \tan\left[\mathrm{JRC}\lg\left(\frac{\mathrm{JCS}}{\sigma_n}\right) + \phi_b\right], \quad (2)$$

where JRC is the joint surface roughness coefficient, JCS is the compressive strength of the joint face wall (MPa), σ_n is the normal stress (MPa) on the joint surface, and ϕ_b is the basic internal friction angle of the joint surface (°).

To quantitatively analyze the correlation between micromorphology and shear strength of the joint surface under dry-wet cycling conditions, we must first obtain the JRC, JCS, and ϕ_b of the joint surface.

Previous studies have shown that the joint surface roughness coefficient JRC is strongly correlated with the slope root mean square S_{dq}. Yang et al. [29] proposed an empirical formula for determining the JRC value based on S_{dq}:

$$\mathrm{JRC} = 32.69 + 32.98\lg S_{dq}. \quad (3)$$

We calculated the roughness coefficient JRC of the joint surface using formula (3). The results are shown in Table 3; the JRC variation pattern is shown in Figure 8.

In addition, we carried out uniaxial compression tests throughout the experiments. The measured uniaxial compressive strength was used as the compressive strength JCS of the joint face wall (as shown in Table 4); the variation curve of JCS is shown in Figure 9.

We also tested the basic internal friction angle ϕ_b of the joint surface (Table 5) and the variation curve of ϕ_b (Figure 10) after different numbers of dry-wet cycles.

According to formula (3), the shear strength of jointed rock masses under dry-wet cycling can be calculated. As shown in Table 6 and Figure 11, the shear strength of the jointed rock masses under different normal stress conditions changes as more dry-wet cycles are completed.

It can be seen from Figure 11 that the shear strength of jointed rock masses under dry-wet cycling conditions declines steeply at first and more gently as the number of cycles increases. This is consistent with the law of the microscopic topography parameters of a joint surface. It shows that the change law describing the shear strength of jointed rock masses is closely related to the micromorphology of the joint surface.

To verify the rationality of the calculated shear strength values of jointed rock masses, we carried out direct shear tests multiple times during the experiment; the test results are shown in Figure 11. As shown, the calculated shear strength of the jointed rock masses is in close agreement with the experimental values. In both cases, the microscopic joint surface gradually becomes flat, the roughness and the degree of undulation gradually decrease, and the surface wall strength and friction performance of the joint surface gradually deteriorate. As a result, the shear strength of the jointed rock masses gradually decreases with increasing numbers of dry-wet cycles.

Table 3: The roughness coefficient JRC of joint surface under dry-wet cycling conditions.

Number of dry-wet cycles (n)	JRC
0	13.4618
1	13.1570
3	12.9766
5	12.8912
8	12.8054
12	12.7248
16	12.6263
20	12.5914

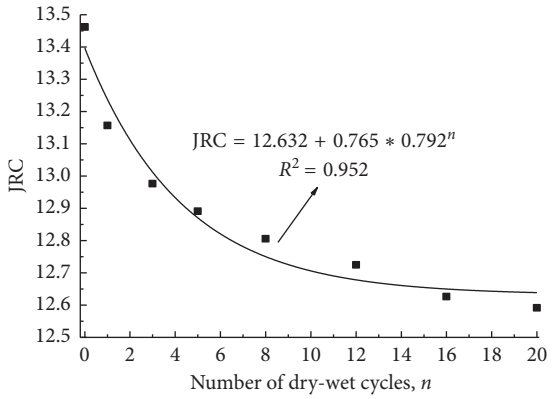

Figure 8: The change curve of the JRC of the joint surface under dry-wet cycling.

Table 4: The compressive strength JCS of joint face wall under dry-wet cycling.

Number of dry-wet cycles (n)	JCS (MPa)
0	68.4452
1	62.9841
3	57.4997
5	48.0213
8	42.4450
12	36.4949
16	31.1361
20	30.2568

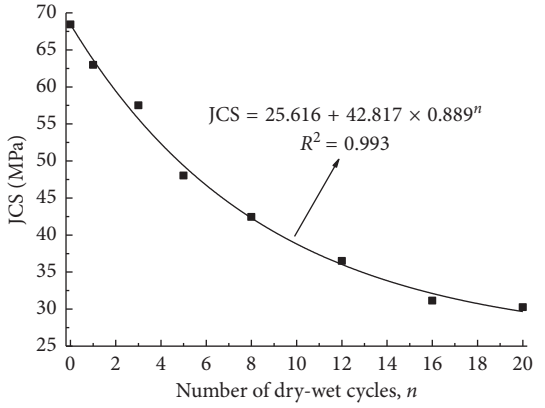

Figure 9: The JCS curve under dry-wet cycling.

Table 5: The basic internal friction angle ϕ_b of joint surface under dry-wet cycling.

Number of dry-wet cycles (n)	ϕ_b (°)
0	27.45
1	27.00
3	26.67
5	26.28
8	25.69
12	25.25
16	25.06
20	25.00

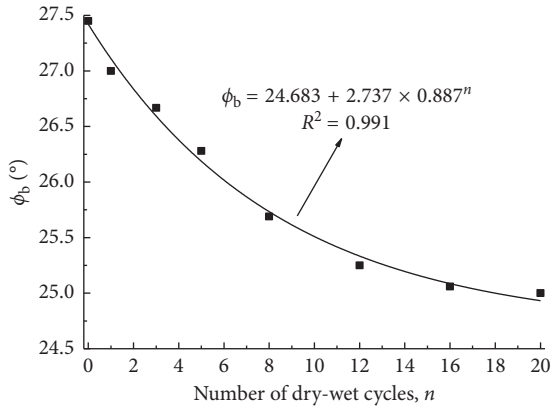

Figure 10: The change curve of JCS of the joint surface under dry-wet cycling.

Table 6: Calculation results for shear strength of jointed rock masses under dry-wet cycling.

Number of dry-wet cycles (n)	Shear strength of jointed rock masses under dry-wet cycling			
	1.0 MPa	1.5 MPa	2.0 MPa	2.5 MPa
0	1.287	1.774	2.229	2.662
1	1.221	1.687	2.123	2.538
3	1.171	1.621	2.042	2.443
5	1.109	1.536	1.936	2.317
8	1.055	1.463	1.844	2.207
12	1.005	1.393	1.757	2.103
16	0.963	1.336	1.685	2.017
20	0.954	1.324	1.670	1.998

5. Analysis of the Mechanism of Joint Surface Deterioration under Dry-Wet Cycling

The sandstone used in the experiments is mainly composed of quartz, feldspar, and rock debris and has porous calcium cementation. In terms of chemical and physical properties, quartz is relatively stable, whereas calcareous cements are prone to corrosion and dissolution under dry-wet cycling. Feldspar minerals are more prone to water-rock physicochemical effects. During soaking, water molecules infiltrate the sandstone.

Under the influence of water, calcareous cements are prone to corrosion and dissolution; water-rock chemistry

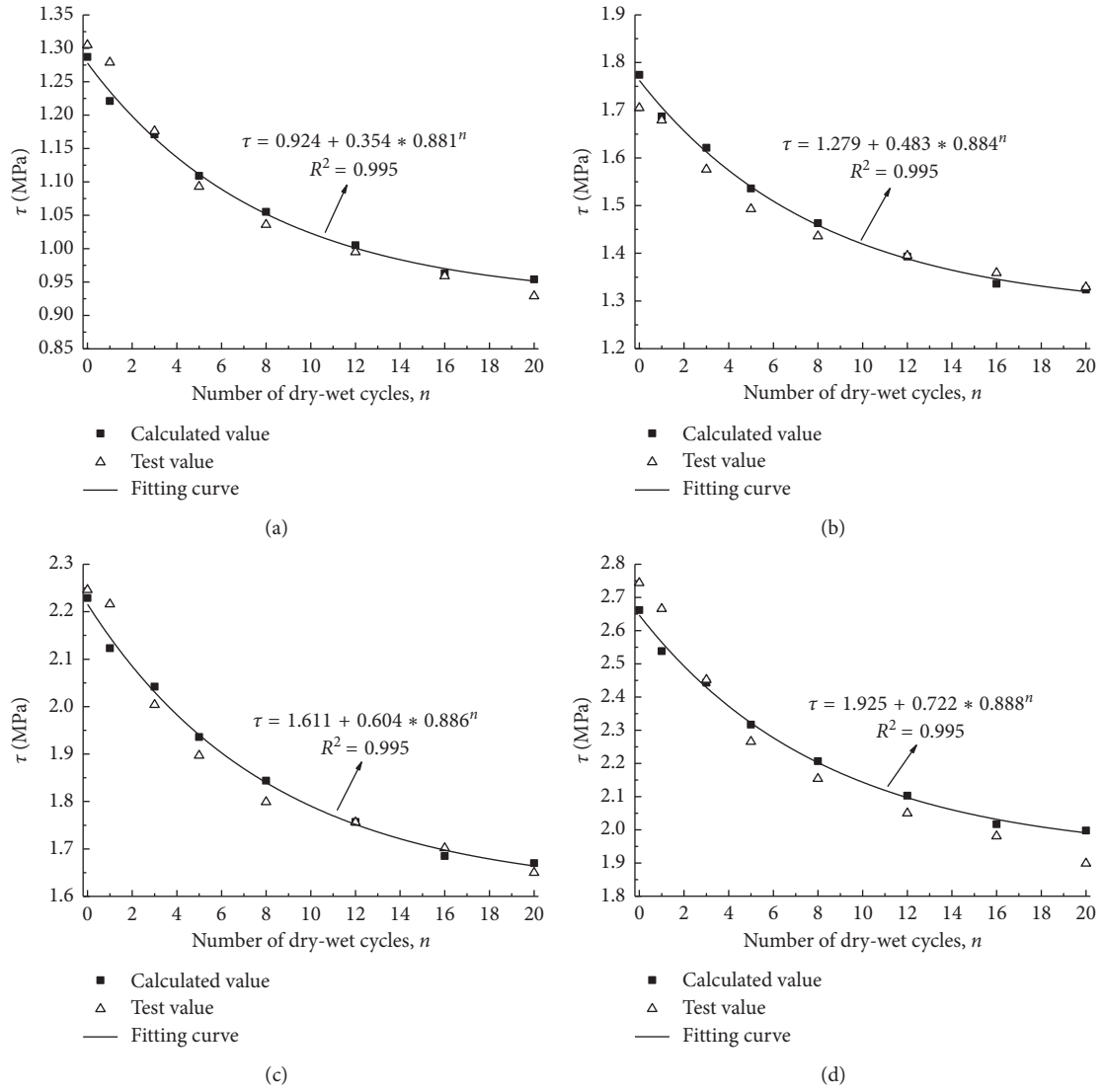

Figure 11: Curve of shear strength of jointed rock masses under dry-wet cycling. (a) Normal stress: 1.0 MPa. (b) Normal stress: 1.5 MPa. (c) Normal stress: 2.0 MPa. (d) Normal stress: 2.5 MPa.

occurs in potassium feldspar, albite, and anorthite, resulting in secondary minerals such as kaolinite [30, 31]. The difference in the volume of space occupied by the body results in inhomogeneous tensioning of the rock mineral particles during stress, which in turn leads to a gradual weakening of the connections between the mineral particles.

Water also has obvious lubricating and softening effects on rock mineral particles and cements, resulting in softening of the mineral particle skeleton. During the drying process, water molecules are extravasated. Due to the uneven distribution of water molecules from the inside to the outside and the nonuniformity of the structure of the rock particles, microscopic cracks are easily generated among the mineral particles, further leading to loosening of the connection between the rock particles. During dry-wet cycling, the repeated infiltration and extravasation of water molecules on the joint surface result in the continuous exfoliation of mineral particles protruding from the joint surface and the gradual smoothing of the particle shape [30, 31]. As a result, the joint surface roughness and degree of undulation gradually decrease, and the shear strength of the jointed rock masses gradually deteriorates.

From the previous test results, the microscopic topography parameters of the joint surface, the compressive strength of the joint wall, and the shear strength all show rapid changes followed by gradual changes as the number of cycles increases. These changes are mainly related to the process of dry-wet cycling at the joint surface. In the early stage of dry-wet cycling (1 to 5 cycles), the dissolution and corrosion rate of calcareous cement materials are faster, and the water-rock chemistry of feldspar minerals develops progressively, resulting in rapid deterioration of microscopic morphology and the shear strength of the joint surface. After 5 dry-wet cycles, the calcareous cement content was reduced significantly. As a result, dissolution was weakened and the ion concentration in the soaking solution reached a relatively high

level, causing the rate of physical/chemical action on the feldspar minerals to slow.

6. Conclusion

(1) Under dry-wet cycling conditions, the height parameters and texture parameters of the joint surface decrease, rapidly at first and then more slowly. Such a trend is best fit by an exponential function. The deterioration of morphology parameters is obvious.

(2) The law of shear strength degradation of jointed rock masses under dry-wet cycling was analyzed based on the microstructural parameters of the joint surface, the compressive strength of the wall, and the basic friction angle. Our calculated results are in good agreement with the experimental results, indicating that the micromorphology and joint wall strength of the joint surface under dry-wet cycling directly affect the shear strength of the jointed rock masses.

(3) The microscopic morphology parameters and the shear strength degradation of the joint surface are not closely synchronized under dry-wet cycling; this is mainly related to the process of dry-wet cycling. The dissolution and dissolution of calcareous cements and the water-rock physicochemical effects of various feldspar minerals result in the deterioration of the microscopic topography and mechanical properties of the joint surface.

Data Availability

The experimental data including figures and tables used to support the findings of this study are included within the article and available from the corresponding author upon request.

Conflicts of Interest

The authors declare that they have no conflicts of interest.

Acknowledgments

This work was supported by the Key Laboratory of Geological Hazards on Three Gorges Reservoir Area (China Three Gorges University), Ministry of Education open fund project (no. 2018KDZ04), and National Nature Science Foundation of China (Grant nos. 51439003 and 51679127).

References

[1] L. F. Shen, X. T. Feng, P. Z. Pan, and H. Zhou, "Experimental research on mechano-hydro-chemical coupling of granite with single fracture," *Chinese Journal of Rock Mechanics and Engineering*, vol. 29, no. 7, pp. 1379–1388, 2010.

[2] P. Li and J. Liu, "Experimental and theoretical studies on the effects of water content on shear creep behavior of weak structural plane of sandstone," *Hydrogeology and Engineering Geology*, vol. 36, no. 6, pp. 49–53+67, 2009.

[3] J. Liu, X. T. Feng, X. L. Ding, and H. M. Zhou, "In situ tests on creep behavior of rock mass with joint or shearing zone in foundation of large-scale hydroelectric projects," *Key Engineering Materials*, vol. 261–263, pp. 1097–1102, 2004.

[4] S. T. Wang, H. C. Liu, Z. Y. Zhang, R. Q. Huang, M. Xu, and Y. Q. Shang, "Study on water-rock interaction and its environmental effects in large-scale waters," *Journal of Geological Hazards and Environment Preservation*, vol. 8, no. 1, pp. 70–90, 1997.

[5] X. R. Liu, Y. Fu, Y. X. Wang, L. W. Huang, and X. Y. Qin, "Deterioration rules of shear strength of sand rock under water-rock interaction of reservoir," *Chinese Journal of Geotechnical Engineering*, vol. 30, no. 9, pp. 1298–1302, 2008.

[6] Z. M. Xu, "The chemical water-rock interaction in silicate rock slopes," *Acta Geologica Sinica*, vol. 87, no. 6, pp. 860–871, 2013.

[7] S. Zhou, X. Q. Liu, M. F. Shang, and Y. Li, "Time-varying stability analysis of mudstone reservoir bank based on water-rock interaction," *Rock and Soil Mechanics*, vol. 33, no. 7, pp. 1933–1939, 2012.

[8] P. A. Hale and A. Shakoor, "A laboratory investigation of the effects of cyclic heating and cooling, wetting and drying, and freezing and thawing on the compressive strength of selected sandstones," *Environmental and Engineering Geoscience*, vol. 9, no. 2, pp. 117–130, 2003.

[9] Y. Fu, X. R. Liu, Y. X. Zhang, Y. X. Hu, and Y. Q. Xie, "Study on the influence of water-rock interaction to the strength of sandstone," *Hydrogeology and Engineering Geology*, vol. 36, no. 6, pp. 54–58, 2009.

[10] Y. Fu, *Study on Water-Rock Interaction with the Cyclic Drying-Wetting Effect on Rock*, Chongqing University, Chongqing, China, 2010.

[11] H. Y. Yao, Z. H. Zhang, C. H. Zhu, Y. H. Shi, and Y. Li, "Experimental study of mechanical properties of sandstone under cyclic drying and wetting," *Rock and Soil Mechanics*, vol. 31, no. 12, pp. 3704–3708, 2010.

[12] Y. D. Jiang, Z. L. Yan, Y. X. Liu, X. Y. Yang, and L. Xiong, "Experimental study on mechanical properties of rock under the conditions of wet and dry cycles," *China Mining Magazine*, vol. 20, no. 5, pp. 104–110, 2011.

[13] Y. Guo, *Research on the Damage Mechanism of Siltstone from Xiangxi River Dank in Drying and Wetting Cycle*, China University of Geosciences, Wuhan, China, 2013.

[14] C. Apollaro, L. Marini, T. Critelli, and R. De Rosa, "The standard thermodynamic properties of vermiculites and prediction of their occurrence during water-rock interaction," *Applied Geochemistry*, vol. 35, no. 4, pp. 264–278, 2013.

[15] M. Tallini, B. Parisse, M. Petitta, and M. Spizzico, "Long-term spatio-temporal hydrochemical and 222Rn tracing to investigate groundwater flow and water-rock interaction in the Gran Sasso (central Italy) carbonate aquifer," *Hydrogeology Journal*, vol. 21, no. 7, pp. 1447–1467, 2013.

[16] P. Alt-Epping, L. W. Diamond, M. O. Häring, F. Ladner, and D. B. Meier, "Prediction of water-rock interaction and porosity evolution in a granitoid-hosted enhanced geothermal system, using constraints from the 5km Basel-1 well," *Applied Geochemistry*, vol. 38, pp. 121–133, 2013.

[17] W. H. Huang, *Study on Deterioration Effect of Sandstone under Alternating Dry-wet Condition*, Kunming University of Science and Technology, Kunming, China, 2014.

[18] J. A. Hurowitz and W. W. Fischer, "Contrasting styles of water-rock interaction at the Mars Exploration Rover landing sites," *Geochimica et Cosmochimica Acta*, vol. 127, no. 3, pp. 25–38, 2014.

[19] K. Cui, G. P. Wu, X. L. Wang, W. W. Chen, and H. M. Lu, "Drying-wetting-saturating experiments for deterioration of

physical and mechanical properties of slate," *Journal of Engineering Geology*, vol. 23, no. 6, pp. 1045–1052, 2015.

[20] M. L. Zhou, *The Creep Mechanism of Red-layer Soft Rock Under Water-rock Interaction at Three Gorges Reservoir Area*, China Three Gorges University, Yichang, China, 2016.

[21] Z. J. Wang, *Damage Evolution Characteristics and The Accumulation Damage Model of Sandstone Under Dry-Wet Cycle*, Chongqing University, Chongqing, China, 2016.

[22] J. Y. Zhang, L. P. Wan, H. Y. Pan, J. L. Li, Z. S. Luo, and H. F. Deng, "Long-term stability of bank slope considering characteristics of water-rock interaction," *Chinese Journal of Geotechnical Engineering*, vol. 39, no. 10, pp. 1851–1858, 2017.

[23] H. F. Deng, X. F. Yuan, and L. H. Wang, "Experimental research on changes in the mechanical property law of reservoir bank sandstone under immersion-air dry circulation," *Environmental Engineering and Management Journal*, vol. 12, no. 9, pp. 1785–1789, 2013.

[24] H. F. Deng, M. L. Zhou, and J. L. Li, "Creep degradation mechanism by water-rock interaction in the red-layer soft rock," *Arabian Journal of Geosciences*, vol. 9, no. 12, pp. 1–12, 2016.

[25] F. S. Jeng, M. L. Lin, and T. H. Huang, "Wetting deterioration of soft sandstone-microscopic insights," in *Proceedings of International Conference on Geotechnical and Geological Engineering*, Melbourne, Australia, November 2000.

[26] M. L. Lin, F. S. Jeng, L. S. Tsai, and T. H. Huang, "Wetting weakening of tertiary sandstones-microscopic mechanism," *Environmental Geology*, vol. 48, no. 2, pp. 265–275, 2005.

[27] Y. Cheng, P. Cao, C. Z. Pu, Y. K. Liu, and N. Li, "Experimental study of effect of water-rock interaction on micro -topography of rock surface," *Rock and Soil Mechanics*, vol. 31, no. 11, pp. 3452–3458, 2010.

[28] M. Q. Shen and J. F. Chen, *Rock Mass Mechanics*, Tongji University Press, Shanghai, China, 2nd edition, 2015.

[29] Z. Y. Yang, S. C. Lo, and C. C. Di, "Reassessing the joint roughness coefficient (JRC) estimation using Z 2," *Rock Mechanics and Rock Engineering*, vol. 34, no. 3, pp. 243–251, 2001.

[30] W. Q. Li, X. P. Zhang, and Y. M. Zhong, "Formation mechanism of secondary dissolved pores in arose," *Oil and Gas Geology*, vol. 26, no. 2, pp. 220–229, 2005.

[31] H. F. Deng, J. L. Li, K. W. Wang, J. Liu, M. Zhu, and T. Lu, "Research on secondary porosity changing law of sandstone under saturation-air dry cycles," *Rock and Soil Mechanics*, vol. 33, no. 2, pp. 483–488, 2012.